Noncoplanarity in proton-proton bremsstrahlung

R. G. E. Timmermans

Theory Group, Kernfysisch Versneller Instituut, University of Groningen, Zernikelaan 25, NL-9747 AA Groningen, The Netherlands

B. F. Gibson

Theoretical Division, Los Alamos National Laboratory, Los Alamos, New Mexico 87545

Yi Li and M. K. Liou

Department of Physics and Institute for Nuclear Theory, Brooklyn College of the City University of New York, Brooklyn, New York 11210

Using the soft-photon approximation, we address the issue of the importance of noncoplanarity effects in proton-proton bremsstrahlung. We investigate the noncoplanar cross section as a function of the noncoplanarity angle $\bar{\phi}$ for the entire range of the photon polar angle ψ_γ. The $\bar{\phi}$ dependence is shown to provide a significant variation in the cross section, for a given ψ_γ. Thus, there can be some uncertainty in determining experimental coplanar cross sections. To avoid the phase-space singularities of spherical geometry, we utilize the Harvard noncoplanar geometry. A detailed explication of the Harvard geometry is provided. Comparison of our calculations with experimental data is included.

PACS number(s): 13.75.Cs, 13.40.−f, 13.60.−r, 11.80.Cr

I. INTRODUCTION

The role of noncoplanarity in proton-proton bremsstrahlung ($pp\gamma$) has recently been highlighted. In a theoretical investigation [1], significant noncoplanarity effects were observed in the differential cross section for certain photon angles ψ_γ. In a high-statistics Kernfysisch Versneller Instituut (KVI) experiment [2–4], coplanar and noncoplanar cross sections were systematically measured. The KVI noncoplanar results [3,4] confirm that noncoplanarity effects are important. In addition, it is stated [4] that noncoplanar cross sections can test models and theoretical approximations in a more sensitive manner than coplanar results. These findings, theoretical and experimental, demonstrate that noncoplanarity contributions should not be neglected.

In the past most experiments measured only the coplanar cross sections, which were then compared with theoretical predictions using various coplanar bremsstrahlung amplitudes. Coplanar amplitudes are clearly missing the dependence upon the noncoplanarity angle $\bar{\phi}$. Moreover, as pointed out in Ref. [1], there is some uncertainty involved in determining experimental coplanar cross sections. This limits what one can learn from any comparison between experiment and theory in the purely coplanar case. Furthermore, one cannot rule out the possibility that noncoplanar effects, not of dynamical origin, are at least partly responsible for some disagreements in past comparisons between theory and experiment. Finally, an important issue has been raised regarding the presentation of coplanar and noncoplanar $pp\gamma$ data, which is to be compared with theoretical calculations [5,6].

Historically, two different experimental arrangements, known as the Harvard geometry and the Rochester geometry, have been used in $pp\gamma$ cross section measurements [7]. The Rochester geometry [8] refers to an experimental arrangement in which the momenta of the two outgoing protons ($p_1'^\mu$ and $p_2'^\mu$) and the emitted photon (K^μ) are detected and

a differential cross section of the form $d^3\sigma/d\Omega_1 d\Omega_\gamma dK$ is measured. (The $p_1'^\mu$, $p_2'^\mu$, and K^μ, and other notation, will be defined in Sec. II.) Here $d\Omega_1$, $d\Omega_2$, and $d\Omega_\gamma$ are the solid angles corresponding to the three momenta $p_1'^\mu$, $p_2'^\mu$, and K^μ, respectively. The photon momentum $\vec{K}$ defines a polar angle θ_γ in the spherical coordinate system and a related polar angle ψ_γ in the Harvard coordinate system. Because very few experiments have used the Rochester geometry, we will focus our remarks on the Harvard geometry [9].

In most experiments employing the Harvard geometry, the momenta $p_1'^\mu$ and $p_2'^\mu$ were measured and the momentum K^μ was inferred using energy-momentum conservation. The differential cross section $d^3\sigma/d\Omega_1 d\Omega_2 d\theta_\gamma$ can be extracted, if the spherical coordinate system is used to analyze the data. However, because the cross section in this form exhibits kinematic singularities near the end points of the range of θ_γ for the noncoplanar case, the Harvard noncoplanar coordinate system [9,10] has been used to measure noncoplanar and coplanar cross sections of the form $d^3\sigma/d\Omega_1 d\Omega_2 d\psi_\gamma$, which is free of such kinematic singularities. The Harvard experiment [9], the Manitoba experiment [11], and the Oak Ridge experiment [12] are three examples of successful measurements using the Harvard geometry. The KVI experiment differs in that all three final-state particles were detected, but cross sections of the form $d^3\sigma/d\Omega_1 d\Omega_2 d\theta_\gamma$ (plus analyzing powers) were measured. There are other experiments [13] in which cross sections and/or analyzing powers were measured using the Harvard geometry.

There is a crucial difference between the Rochester geometry (cross section of the form $d^3\sigma/d\Omega_1 d\Omega_\gamma dK$) and the Harvard geometry (cross section of the form $d^3\sigma/d\Omega_1 d\Omega_2 d\theta_\gamma$ or $d^3\sigma/d\Omega_1 d\Omega_2 d\psi_\gamma$). In the Rochester geometry, the photon energy K is an independent kinematic variable, and its range includes the point $K=0$. In the Harvard geometry, in contrast, K is a dependent variable and its range does not include the point $K=0$ *except* in the elastic

65 014001-1

limit. One implication of this difference lies in the interpretation of the soft-photon theorem and the soft-photon expansion, which is discussed in the Appendix.

Recently, progress has been achieved in the theoretical investigation of $pp\gamma$. Sophisticated calculations, using either contemporary nucleon-nucleon potentials or other approaches, have been performed [14]. Higher-order effects such as rescattering terms, relativistic spin corrections, negative-energy states, Δ-isobar admixtures, electromagnetic form factors, higher-order exchange currents, and the difference between pseudoscalar and pseudovector πN couplings in low order have been explored. However, much less attention has been given to noncoplanarity effects and to their role in interpreting experimental coplanar cross sections. In Ref. [1], we investigated these problems using two different approaches, a soft-photon approximation based upon a two-u–two-t special ($TuTts$) amplitude [15,16] and a realistic one-boson-exchange model [17]. As shown in Fig. 1 of Ref. [1], those two approaches lead to similar predictions. More recently, the $TuTts$ amplitude has been tested by comparison with KVI experimental data [2–4]. The validity of its use in describing the $pp\gamma$ cross section has been well established. This encourages us to employ the $TuTts$ amplitude in further exploration of noncoplanarity effects. We report here on additional results of our soft-photon calculations, provide the details of our method, present explicit expressions for the Harvard geometry kinematics, and compare to the available experimental data.

This paper is organized as follows. We discuss in Sec. II the kinematics defined in the Harvard noncoplanar system. We present a complete set of formulas which can be used to determine the needed coordinates for noncoplanar calculations. In Sec. III we define the pp elastic scattering amplitude which is used to generate the $TuTts$ bremsstrahlung amplitude. We give explicit expressions for the $TuTts$ amplitude along with comments about its evaluation. In Sec. IV we present numerical results and discuss their implications. In the Appendix we address certain subtleties of the soft-photon approximation.

II. KINEMATICS

A. The Harvard noncoplanar geometry

We consider the $pp\gamma$ process,

$$p(p_1^\mu) + p(p_2^\mu) \rightarrow p(p_1'^\mu) + p(p_2'^\mu) + \gamma(K^\mu), \quad (1)$$

where $p_1^\mu(p_2^\mu)$ is the four-momentum of the incident (target) proton, $p_1'^\mu(p_2'^\mu)$ is the four-momentum of the scattered (recoil) proton, and K^μ is the four-momentum of the emitted photon with polarization ϵ^μ. In the spherical coordinate system a three-momentum can be specified by the polar angle θ and the azimuthal angle ϕ, while in the Harvard coordinate system the momentum is specified by two Harvard angles $\bar{\theta}$ and $\bar{\phi}$. (We follow the Harvard noncoplanar approach as outlined in the Appendix of Ref. [10].) The angles θ, ϕ, $\bar{\theta}$, and $\bar{\phi}$ are defined relative to the x-z reference plane as

shown in Fig. 15 of Ref. [10]. In the Harvard coordinate system the momenta p_1^μ, p_2^μ, $p_1'^\mu$, $p_2'^\mu$, and K^μ have the following components:

$$p_1^\mu = (E_1, 0, 0, p_1),$$

$$p_2^\mu = (m, 0, 0, 0),$$

$$p_1'^\mu = (E_1', p_1' \cos\bar{\phi}_1 \sin\bar{\theta}_1, p_1' \sin\bar{\phi}_1, p_1' \cos\bar{\phi}_1 \cos\bar{\theta}_1),$$

$$p_2'^\mu = (E_2', -p_2' \cos\bar{\phi}_2 \sin\bar{\theta}_2, p_2' \sin\bar{\phi}_2, p_2' \cos\bar{\phi}_2 \cos\bar{\theta}_2),$$

$$K^\mu = (K, K \cos\bar{\phi}_\gamma \sin\bar{\theta}_\gamma, -K \sin\bar{\phi}_\gamma, K \cos\bar{\phi}_\gamma \cos\bar{\theta}_\gamma),$$

$$(2)$$

where

$$E_1 = \sqrt{m^2 + \vec{p}_1^2} = m + T_1,$$

$$E_1' = \sqrt{m^2 + \vec{p}_1'^2} = m + T_1',$$

$$E_2' = \sqrt{m^2 + \vec{p}_2'^2} = m + T_2', \quad (3)$$

and m is the proton mass. The proton has charge e and anomalous magnetic moment $\kappa = 1.793$. The relation between the coordinates in spherical and Harvard geometry reads

$$\phi_1 = \tan^{-1}[\csc\bar{\theta}_1 \tan\bar{\phi}_1],$$

$$\phi_2 = \pi - \tan^{-1}[\csc\bar{\theta}_2 \tan\bar{\phi}_2],$$

$$\phi_\gamma = 2\pi - \tan^{-1}[\csc\bar{\theta}_\gamma \tan\bar{\phi}_\gamma],$$

$$\theta_i = \tan^{-1}[\tan^2\bar{\theta}_i + \sec^2\bar{\theta}_i \tan^2\bar{\phi}_i]^{1/2}, \quad (i=1,2,\gamma). \quad (4)$$

For coplanar events, the three noncoplanarity angles, $\bar{\phi}_i$ ($i=1,2,\gamma$), vanish and Eqs. (4) become

$$\phi_1 = 0,$$

$$\phi_2 = \pi,$$

$$\phi_\gamma = 2\pi,$$

$$\theta_i = \bar{\theta}_i, \quad (i=1,2,\gamma). \quad (5)$$

For a given incident kinetic energy T_1, there are three outgoing particles with nine kinematic degrees of freedom. Because energy and momentum are conserved,

$$p_1^\mu + p_2^\mu = p_1'^\mu + p_2'^\mu + K^\mu, \quad (6)$$

only five of the kinematic variables are independent. The choice of these five independent variables depends on the experimental arrangement. For example, in terms of the spherical coordinate system we can choose the set $(\theta_1, \phi_1, \theta_2, \phi_2, \theta_\gamma)$ to be independent variables and express the differential cross section in the form $d^3\sigma/d\Omega_1 d\Omega_2 d\theta_\gamma$. Or, in terms of the Harvard coordinate system, we can

choose the set $(\bar{\theta}_1, \bar{\phi}_1, \bar{\theta}_2, \bar{\phi}_2, \bar{\theta}_\gamma)$ to be independent variables and express the differential cross section in the form $d^3\sigma/d\bar{\Omega}_1 d\bar{\Omega}_2 d\bar{\theta}_\gamma$. Note that the solid angles $d\Omega_i$ and $d\bar{\Omega}_i$ ($i=1,2$) are defined as

$$d\Omega_i = \sin\theta_i \, d\theta_i \, d\phi_i,$$

$$d\bar{\Omega}_i = \cos\bar{\phi}_i \, d\bar{\theta}_i \, d\bar{\phi}_i. \tag{7}$$

Because it can be shown that

$$\sin\theta_i \, d\theta_i \, d\phi_i = \cos\bar{\phi}_i \, d\bar{\theta}_i \, d\bar{\phi}_i, \tag{8}$$

we have $d\bar{\Omega}_i = d\Omega_i$, and hence

$$d^3\sigma/d\bar{\Omega}_1 d\bar{\Omega}_2 d\bar{\theta}_\gamma = d^3\sigma/d\Omega_1 d\Omega_2 d\bar{\theta}_\gamma. \tag{9}$$

In the coplanar case the cross section $d^3\sigma/d\Omega_1 d\Omega_2 d\theta_\gamma$ ($\bar{\theta}_\gamma = \theta_\gamma$) has no kinematic singularity in the entire photon range ($0 \leq \theta_\gamma \leq 2\pi$). However, for noncoplanar events the allowed range for θ_γ (or $\bar{\theta}_\gamma$) shrinks to less than 2π and the cross section $d^3\sigma/d\Omega_1 d\Omega_2 d\theta_\gamma$ (or $d^3\sigma/d\Omega_1 d\Omega_2 d\bar{\theta}_\gamma$) diverges at the extreme photon emission angles due to the phase-space factor. This problem can be avoided by introducing the special photon polar angle ψ_γ in the Harvard noncoplanar coordinate system.

Two steps are involved in defining this new angle ψ_γ. (i) The first step is to define the so-called "limiting γ ray." In the Harvard geometry, the average noncoplanar angle of the protons, $\bar{\phi} = (\bar{\phi}_1 + \bar{\phi}_2)/2$, has a kinetically allowed maximum, which we call $\bar{\phi}_{max}$. The corresponding emitted photon is called the limiting γ ray. It has a three-momentum $\vec{K}_0$ specified by two special Harvard angles, $\bar{\theta}_0$ and $\bar{\phi}_0$:

$$\vec{K}_0 = (K_0 \cos\bar{\phi}_0 \sin\bar{\theta}_0, -K_0 \sin\bar{\phi}_0, K_0 \cos\bar{\phi}_0 \cos\bar{\theta}_0). \tag{10}$$

(ii) As shown in Fig. 1, a new coplanar photon momentum $\vec{K}'$ in the x-z reference plane can be defined by a vector sum of $\vec{K}$ and $-\alpha\vec{K}_0$,

$$\vec{K}' \equiv \vec{K} - \alpha\vec{K}_0. \tag{11}$$

The polar angle of this new photon momentum is ψ_γ, where

$$\vec{K}' = (K' \sin\psi_\gamma, 0, K' \cos\psi_\gamma). \tag{12}$$

We obtain from Eq. (11)

$$\tan\psi_\gamma = \frac{\sin\bar{\theta}_\gamma - \cot\bar{\phi}_0 \tan\bar{\phi}_\gamma \sin\bar{\theta}_0}{\cos\bar{\theta}_\gamma - \cot\bar{\phi}_0 \tan\bar{\phi}_\gamma \cos\bar{\theta}_0}. \tag{13}$$

If we choose the set $(\bar{\theta}_1, \bar{\phi}_1, \bar{\theta}_2, \bar{\phi}_2, \psi_\gamma)$ as the independent kinematic variables, the cross section $d^3\sigma/d\Omega_1 d\Omega_2 d\psi_\gamma$ has no kinematic singularity in the range $0 \leq \psi_\gamma \leq 2\pi$. One has mapped the allowed range of $\bar{\theta}_\gamma$, which is less than 2π, onto the full 2π range of ψ_γ. Among the advantages of this

FIG. 1. Three-dimensional representation of the momentum vectors required in defining the new coplanar photon momentum $\vec{K}'$ and its polar angle ψ_γ in the Harvard geometry. In the figure $\vec{K}$ is the original photon momentum, $\vec{K}_0$ is the limiting γ ray, and α is a constant.

choice of variables, one can integrate this cross section over ψ_γ to obtain $d^2\sigma/d\Omega_1 d\Omega_2$ with no difficulty. In the coplanar case ψ_γ reduces to θ_γ and $d^3\sigma/d\Omega_1 d\Omega_2 d\psi_\gamma$ becomes $d^3\sigma/d\Omega_1 d\Omega_2 d\theta_\gamma$. In this work, we calculate $d^3\sigma/d\Omega_1 d\Omega_2 d\psi_\gamma$ as a function of ψ_γ, $\bar{\phi}$, and T_1.

Finding the limiting angles $\bar{\phi}_{max}$, $\bar{\theta}_0$, and $\bar{\phi}_0$ is one of the complicated steps in calculating the noncoplanar cross section, especially for the asymmetric case $\bar{\theta}_1 \neq \bar{\theta}_2$. Various methods can be used to determine these angles. For example, using the simple method of Lagrange multipliers one can derive two coupled equations for the proton momenta $\tilde{p}_1'$ and $\tilde{p}_2'$. After solving these two nonlinear equations numerically, one may then calculate the angles $\bar{\phi}_{max}$, $\bar{\theta}_0$, and $\bar{\phi}_0$ from $\tilde{p}_1'$, $\tilde{p}_2'$, and other given conditions. Details are discussed in the next subsection.

B. The limiting gamma ray

If we choose a common noncoplanarity angle $\bar{\phi}$ for the two outgoing protons ($\bar{\phi} = \bar{\phi}_1 = \bar{\phi}_2$), then $\bar{\phi}$ has a maximum value, $\bar{\phi}_{max}$. At this limit, the limiting γ ray is defined and it has momentum $\vec{K}_0 \equiv \vec{K}_0(K_0, \bar{\theta}_0, \bar{\phi}_0)$ given by Eq. (10). If the magnitudes of the two proton momenta $\vec{p}_1'$ and $\vec{p}_2'$ are $\tilde{p}_1'$ and $\tilde{p}_2'$, respectively, at this limit, then we can obtain the following two coupled equations for $\tilde{p}_1'$ and $\tilde{p}_2'$:

$$0 = 2f_1 f_3 \tilde{p}_2'^3 + p_1 \tilde{E}_2' f_4 \cos\bar{\theta}_1$$
$$- \tilde{E}_2' [p_1^2 f_2 \cos\bar{\theta}_1 + \tilde{p}_2' f_3 (p_1^2 + \tilde{p}_1'^2 - \tilde{p}_2'^2 - f_1^2)], \tag{14}$$

$$0 = 2f_1 f_3 \tilde{p}_1'^3 + p_1 \tilde{E}_1' f_4 \cos \bar{\theta}_2$$
$$- \tilde{E}_1'[p_1^2 f_2 \cos \bar{\theta}_2 + \tilde{p}_1' f_3(p_1^2 + \tilde{p}_2'^2 - \tilde{p}_1'^2 - f_1^2)],$$

$$(15)$$

where p_1, f_1, f_2, f_3, f_4, $\tilde{E}_1'$, and $\tilde{E}_2'$ are defined as

$$p_1 = \sqrt{2mT_1 + T_1^2},$$

$$f_1 \equiv f_1(\tilde{p}_1', \tilde{p}_2') = 2m + T_1 - \sqrt{m^2 + \tilde{p}_1'^2} - \sqrt{m^2 + \tilde{p}_2'^2},$$

$$f_2 \equiv f_2(\tilde{p}_1', \tilde{p}_2', \bar{\theta}_1, \bar{\theta}_2) = \tilde{p}_1' \cos \bar{\theta}_1 + \tilde{p}_2' \cos \bar{\theta}_2,$$

$$f_3 \equiv f_3(\bar{\theta}_1, \bar{\theta}_2) = 1 - \cos(\bar{\theta}_1 + \bar{\theta}_2),$$

$$f_4 \equiv f_4(\tilde{p}_1', \tilde{p}_2', \bar{\theta}_1, \bar{\theta}_2)$$
$$= \{p_1^2 f_2^2 + 2\tilde{p}_1' \tilde{p}_2' f_3[p_1^2 + (\tilde{p}_1' + \tilde{p}_2')^2 - f_1^2]\}^{1/2},$$

$$\tilde{E}_1' = \sqrt{m^2 + \tilde{p}_1'^2},$$

$$\tilde{E}_2' = \sqrt{m^2 + \tilde{p}_2'^2}. \quad (16)$$

Using T_1, $\bar{\theta}_1$, $\bar{\theta}_2$, and the values of $\tilde{p}_1'$ and $\tilde{p}_2'$ obtained by solving Eqs. (14) and (15), the values of f_1, f_2, f_3, and f_4 can be found from Eq. (16). These values can be used to determine K_0, $\bar{\phi}_{max}$ ($0 \leq \bar{\phi}_{max} \leq \pi/2$), $\bar{\theta}_0$ ($-\pi/2 \leq \bar{\theta}_0 \leq \pi/2$), and $\bar{\phi}_0$ ($0 \leq \bar{\phi}_0 \leq \pi/2$) as

$$K_0 = f_1, \quad (17)$$

$$\bar{\phi}_{max} = \cos^{-1}[(-p_1 f_2 + f_4)/(2\tilde{p}_1' \tilde{p}_2' f_3)], \quad (18)$$

$$\bar{\theta}_0 = \tan^{-1}[(\tilde{p}_2' \sin \bar{\theta}_2 - \tilde{p}_1' \sin \bar{\theta}_1)$$
$$\times \cos \bar{\phi}_{max}/(p_1 - f_2 \cos \bar{\phi}_{max})], \quad (19)$$

$$\bar{\phi}_0 = \sin^{-1}[(\tilde{p}_1' + \tilde{p}_2') \sin \bar{\phi}_{max}/K_0]. \quad (20)$$

For the symmetric case, one has $\bar{\theta}_1 = \bar{\theta}_2 = \bar{\theta}$, $\bar{\phi}_1 = \bar{\phi}_2 = \bar{\phi}$, $\tilde{p}_1' = \tilde{p}_2' = \tilde{p}'$, and $\bar{\theta}_0 = 0$. In this case, the coupled equations for $\tilde{p}_1'$ and $\tilde{p}_2'$ given by Eqs. (14) and (15) reduce to one single equation of the form

$$0 = 2\tilde{p}'^2(2m + T_1) \sin^2 \bar{\theta} - \sqrt{m^2 + \tilde{p}'^2}$$
$$\times \{p_1^2 \cos^2 \bar{\theta} + \sin^2 \bar{\theta}[p_1^2 + 4\tilde{p}'^2$$
$$- (2m + T_1 - 2\sqrt{m^2 + \tilde{p}'^2})^2]\} + p_1 \sqrt{m^2 + \tilde{p}'^2} \cos \bar{\theta}$$
$$\times \{p_1^2 \cos^2 \bar{\theta} + \sin^2 \bar{\theta}[p_1^2 + 4\tilde{p}'^2$$
$$- (2m + T_1 - 2\sqrt{m^2 + \tilde{p}'^2})^2]\}^{1/2}. \quad (21)$$

After solving this equation numerically to find $\tilde{p}'$, we can calculate K_0, $\bar{\phi}_{max}$, and $\bar{\phi}_0$ from Eqs. (17), (18), and (20), respectively.

Next we can calculate $(p_1', p_2', K, \bar{\theta}_\gamma, \bar{\phi}_\gamma)$ if $(m, T_1, \bar{\theta}_1, \bar{\theta}_2, \bar{\phi}, \psi_\gamma, \bar{\theta}_0, \bar{\phi}_0)$ are given. Once $(p_1', p_2', K, \bar{\theta}_\gamma, \bar{\phi}_\gamma)$ are determined, the complete expressions for $\vec{p}_1'$, $\vec{p}_2'$, and $\vec{K}$ can easily be obtained. Let us first define the following functions of $\bar{\theta}_\gamma$:

$$\tan \bar{\phi}_\gamma = \tan \bar{\phi}_0 \left(\frac{\cos \bar{\theta}_\gamma - \sin \bar{\theta}_\gamma \cot \psi_\gamma}{\cos \bar{\theta}_0 - \sin \bar{\theta}_0 \cot \psi_\gamma} \right), \quad (22)$$

$$\Delta_1(\bar{\theta}_\gamma) = p_1 \begin{vmatrix} -\cos \bar{\phi} \sin \bar{\theta}_2 & \sin \bar{\theta}_\gamma \\ \sin \bar{\phi} & -\tan \bar{\phi}_\gamma \end{vmatrix}, \quad (23)$$

$$\Delta_2(\bar{\theta}_\gamma) = -p_1 \begin{vmatrix} \cos \bar{\phi} \sin \bar{\theta}_1 & \sin \bar{\theta}_\gamma \\ \sin \bar{\phi} & -\tan \bar{\phi}_\gamma \end{vmatrix}, \quad (24)$$

$$\Delta_\gamma(\bar{\theta}_\gamma) = p_1 \sin \bar{\phi} \cos \bar{\phi}(\sin \bar{\theta}_1 + \sin \bar{\theta}_2) \sqrt{1 + \tan^2 \bar{\phi}_\gamma}, \quad (25)$$

$$\Delta(\bar{\theta}_\gamma) = \begin{vmatrix} \cos \bar{\phi} \sin \bar{\theta}_1 & -\cos \bar{\phi} \sin \bar{\theta}_2 & \sin \bar{\theta}_\gamma \\ \sin \bar{\phi} & \sin \bar{\phi} & -\tan \bar{\phi}_\gamma \\ \cos \bar{\phi} \cos \bar{\theta}_1 & \cos \bar{\phi} \cos \bar{\theta}_2 & \cos \bar{\theta}_\gamma \end{vmatrix}, \quad (26)$$

$$p_1'(\bar{\theta}_\gamma) = \frac{\Delta_1(\bar{\theta}_\gamma)}{\Delta(\bar{\theta}_\gamma)}, \quad (27)$$

$$p_2'(\bar{\theta}_\gamma) = \frac{\Delta_2(\bar{\theta}_\gamma)}{\Delta(\bar{\theta}_\gamma)}, \quad (28)$$

$$K(\bar{\theta}_\gamma) = \frac{\Delta_\gamma(\bar{\theta}_\gamma)}{\Delta(\bar{\theta}_\gamma)}. \quad (29)$$

Inserting $p_1'(\bar{\theta}_\gamma)$, $p_2'(\bar{\theta}_\gamma)$, and $K(\bar{\theta}_\gamma)$ into

$$2m + T_1 = \sqrt{m^2 + [p_1'(\bar{\theta}_\gamma)]^2} + \sqrt{m^2 + [p_2'(\bar{\theta}_\gamma)]^2} + K(\bar{\theta}_\gamma) \quad (30)$$

leads to an equation for $\bar{\theta}_\gamma$. Equation (30) can be solved numerically for $\bar{\theta}_\gamma$. Substituting the value of $\bar{\theta}_\gamma$ into Eqs. (22)–(26), we obtain $\bar{\phi}_\gamma$, p_1', p_2', and K from Eqs. (22), (27), (28), and (29), respectively.

Using p_1' and p_2' obtained in Eqs. (27) and (28), respectively, T_1' and T_2' can be calculated from Eq. (3). If $(T_1, \bar{\theta}_1, \bar{\theta}_2, \bar{\phi})$ are given, T_1' and T_2' will be functions of ψ_γ. By varying ψ_γ throughout its entire 2π range, the kinematically allowed values of T_1' and T_2' will form a closed ring in the T_1', T_2' plane. This is the $T_1' - T_2'$ plot; see Ref. [9]. In Figs. 2 and 3, we show these plots for 190 MeV and the symmetric angle pair 16°-16°, and for 280 MeV and the
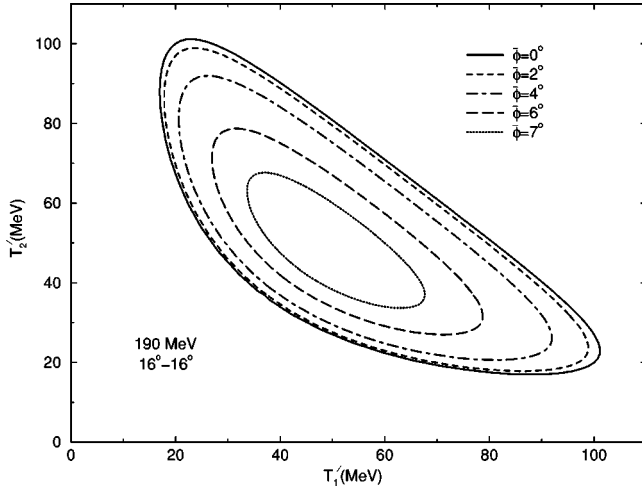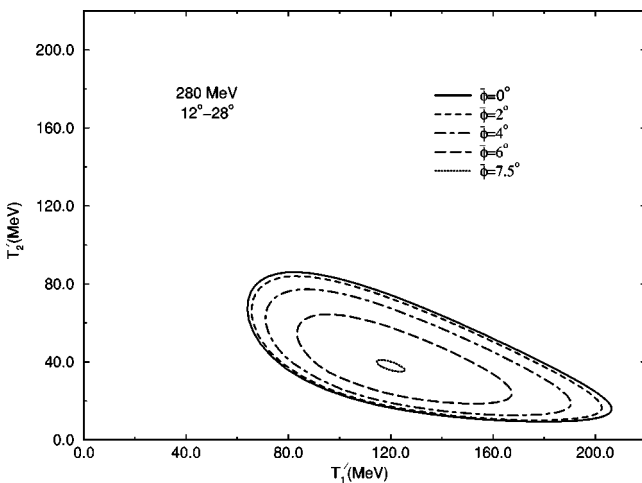
FIG. 2. The kinematically allowed values of T_1' and T_2' as a function of the noncoplanarity angle $\bar{\phi}$ for the KVI energy of 190 MeV and the symmetric angle pair 16°-16°.

asymmetric angle pair 12°-28°, respectively. Starting from the largest ring for the coplanar ($\bar{\phi}=0$) case, as shown in Figs. 2 and 3, these rings become smaller as $\bar{\phi}$ increases. The smallest ring corresponds to $\bar{\phi}$ near the limiting $\bar{\phi}_{max}$. Similar plots were used in the original Harvard experimental analysis and have been used in many other experiments for data analysis.

III. THE PROTON-PROTON BREMSSTRAHLUNG AMPLITUDE

A. The proton-proton elastic scattering amplitude

From the variables in Eq. (1) that describe the $pp\gamma$ process, it is useful to define the following Mandelstam variables:

FIG. 3. The kinematically allowed values of T_1' and T_2' as a function of the noncoplanarity angle $\bar{\phi}$ for the TRIUMF energy of 280 MeV and the asymmetric angle pair 12°-28°.

$$s_i=(p_1+p_2)^2, \quad s_f=(p_1'+p_2')^2,$$

$$t_1=(p_1'-p_1)^2, \quad t_2=(p_2'-p_2)^2,$$

$$u_1=(p_2'-p_1)^2, \quad u_2=(p_1'-p_2)^2. \tag{31}$$

When the photon momentum K approaches zero, the $pp\gamma$ process reduces to the corresponding pp elastic scattering process,

$$p(p_1^\mu)+p(p_2^\mu)\rightarrow p(\bar{p}_1'^\mu)+p(\bar{p}_2'^\mu), \tag{32}$$

where

$$\bar{p}_1'^\mu=\lim_{K\rightarrow 0}p_1'^\mu,$$

$$\bar{p}_2'^\mu=\lim_{K\rightarrow 0}p_2'^\mu, \tag{33}$$

and the Mandelstam variables defined above become

$$s=s_i=(p_1+p_2)^2,$$

$$t=(\bar{p}_1'-p_1)^2=(\bar{p}_2'-p_2)^2,$$

$$u=(\bar{p}_2'-p_1)^2=(\bar{p}_1'-p_2)^2. \tag{34}$$

They satisfy the on-shell condition,

$$s+t+u=4m^2, \tag{35}$$

which shows that only two of the variables are independent.

The representation of the covariant on-shell NN scattering amplitude has been discussed by Goldberger, Grisaru, MacDowell, and Wong (GGMW) [18]. The GGMW amplitude for pp elastic scattering has the form [15]

$$F=F_1(G_1-\tilde{G}_1)+F_2(G_2+\tilde{G}_2)+F_3(G_3-\tilde{G}_3)$$

$$+F_4(G_4+\tilde{G}_4)+F_5(G_5-\tilde{G}_5)$$

$$=\sum_{\alpha=1}^{5}F_\alpha[G_\alpha+(-1)^\alpha\tilde{G}_\alpha], \tag{36}$$

where

$$G_\alpha=\bar{u}(\bar{p}_1')\lambda_\alpha u(p_1)\bar{u}(\bar{p}_2')\lambda^\alpha u(p_2),$$

$$\tilde{G}_\alpha=\bar{u}(\bar{p}_2')\lambda_\alpha u(p_1)\bar{u}(\bar{p}_1')\lambda^\alpha u(p_2), \tag{37}$$

and we define

$$(\lambda_1,\lambda_2,\lambda_3,\lambda_4,\lambda_5)=\left(1,\frac{\sigma_{\mu\nu}}{\sqrt{2}},i\gamma_5\gamma_\mu,\gamma_\mu,\gamma_5\right),$$

$$(\lambda^1,\lambda^2,\lambda^3,\lambda^4,\lambda^5)=\left(1,\frac{\sigma^{\mu\nu}}{\sqrt{2}},i\gamma_5\gamma^\mu,\gamma^\mu,\gamma_5\right). \tag{38}$$

Note that λ_α and λ^α are tensors. For example, $\lambda^2\lambda_2=\lambda_2\lambda^2=\frac{1}{2}\sigma_{\mu\nu}\sigma^{\mu\nu}$, where the summation over μ and ν is implied. In Eq. (36), F_α ($\alpha=1,\ldots,5$) are invariant functions of two

independent Mandelstam variables. Guided by a meson-exchange theory of the NN interaction, we choose u and t to be the two independent variables and we write $F_\alpha = F_\alpha(u,t)$. [For the pp elastic scattering case, $F_\alpha(u,t) = F_\alpha(s,t)$. However, as will discuss below, this relationship is not true for the $pp\gamma$ case.] By imposing the condition

$$F_\alpha(u,t) = (-1)^{\alpha+1} F_\alpha(t,u), \qquad (39)$$

one can verify that the amplitude F given by Eq. (36) obeys the Pauli principle.

B. The two-u−two-t special amplitude

The $TuTts$ amplitude used in our bremsstrahlung calculations is given by the following expression [15]:

$$M_\mu^{TuTts}(u_1,u_2;t_1,t_2)$$

$$= e \sum_{\alpha=1}^{5} [\bar{u}(p_1')X_{\alpha\mu}u(p_1)\bar{u}(p_2')\lambda^\alpha u(p_2)$$

$$+ \bar{u}(p_1')\lambda_\alpha u(p_1)\bar{u}(p_2')Y_\mu^\alpha u(p_2)$$

$$+ \bar{u}(p_2')\lambda^\alpha u(p_1)\bar{u}(p_1')Z_{\alpha\mu}u(p_2)$$

$$+ \bar{u}(p_2')T_\mu^\alpha u(p_1)\bar{u}(p_1')\lambda_\alpha u(p_2)], \qquad (40)$$

where

$$X_{\alpha\mu} = F_\alpha(u_1,t_2)\left[\frac{p_{1\mu}' + R_{1\mu}'}{p_1'\cdot K} - V_\mu\right]\lambda_\alpha$$

$$- F_\alpha(u_2,t_2)\lambda_\alpha\left[\frac{p_{1\mu} + R_{1\mu}}{p_1\cdot K} - V_\mu\right],$$

$$Y_\mu^\alpha = F_\alpha(u_2,t_1)\left[\frac{p_{2\mu}' + R_{2\mu}'}{p_2'\cdot K} - V_\mu\right]\lambda^\alpha$$

$$- F_\alpha(u_1,t_1)\lambda^\alpha\left[\frac{p_{2\mu} + R_{2\mu}}{p_2\cdot K} - V_\mu\right], \qquad (41)$$

$$Z_{\alpha\mu} = (-1)^\alpha F_\alpha(u_1,t_2)\left[\frac{p_{1\mu}' + R_{1\mu}'}{p_1'\cdot K} - V_\mu\right]\lambda_\alpha$$

$$- (-1)^\alpha F_\alpha(u_1,t_1)\lambda_\alpha\left[\frac{p_{2\mu} + R_{2\mu}}{p_2\cdot K} - V_\mu\right],$$

$$T_\mu^\alpha = (-1)^\alpha F_\alpha(u_2,t_1)\left[\frac{p_{2\mu}' + R_{2\mu}'}{p_2'\cdot K} - V_\mu\right]\lambda^\alpha$$

$$- (-1)^\alpha F_\alpha(u_2,t_2)\lambda^\alpha\left[\frac{p_{1\mu} + R_{1\mu}}{p_1\cdot K} - V_\mu\right], \qquad (42)$$

with

$$V_\mu = \frac{(p_1' - p_2)_\mu}{2(p_1' - p_2)\cdot K} + \frac{(p_1' - p_1)_\mu}{2(p_1' - p_1)\cdot K}$$

$$= \frac{(p_1 - p_2')_\mu}{2(p_1 - p_2')\cdot K} + \frac{(p_2 - p_2')_\mu}{2(p_2 - p_2')\cdot K} \qquad (43)$$

and

$$R_{i\mu} = \frac{1}{4}[\gamma_\mu, \not{K}] + \frac{\kappa}{8m}\{[\gamma_\mu, \not{K}], \not{p}_i\},$$

$$R_{i\mu}' = \frac{1}{4}[\gamma_\mu, \not{K}] + \frac{\kappa}{8m}\{[\gamma_\mu, \not{K}], \not{p}_i'\}, \quad (i=1,2). \quad (44)$$

In Eq. (44), we have employed the usual $[A,B] \equiv AB - BA$ and $\{A,B\} \equiv AB + BA$. As shown in Ref. [15], this $TuTts$ amplitude is gauge invariant, obeys the Pauli principle, and satisfies other theoretical constraints.

The amplitude $M_\mu^{TuTts}(u_1,u_2;t_1,t_2)$ is called the two-u−two-t amplitude because it depends on u_1, u_2, t_1, and t_2. It is "special" primarily because it does *not* depend upon a specific linear combination of u_1 and u_2,

$$u_{\bar{\alpha},\bar{\beta}} = \frac{\bar{\alpha}u_1 + \bar{\beta}u_2}{\bar{\alpha} + \bar{\beta}}, \quad \bar{\alpha} \neq 0, \quad \bar{\beta} \neq 0, \qquad (45)$$

and/or the linear combination of t_1 and t_2,

$$t_{\bar{\alpha}',\bar{\beta}'} = \frac{\bar{\alpha}'t_1 + \bar{\beta}'t_2}{\bar{\alpha}' + \bar{\beta}'}, \quad \bar{\alpha}' \neq 0, \quad \bar{\beta}' \neq 0. \qquad (46)$$

Equations (41) and (42) show that $F_\alpha(u_i,t_j)$ $(i,j=1,2)$ are the input for the amplitude M_μ^{TuTts}. In order to treat $F_\alpha(u_i,t_j)$ as on-shell amplitudes, we have to impose on-shell conditions. From the four relations

$$s_i + u_2 + t_1 = 4m^2 + 2p_2'\cdot K, \qquad (47a)$$

$$s_i + u_1 + t_2 = 4m^2 + 2p_1'\cdot K, \qquad (47b)$$

$$s_f + u_2 + t_2 = 4m^2 - 2p_1\cdot K, \qquad (47c)$$

$$s_f + u_1 + t_1 = 4m^2 - 2p_2\cdot K, \qquad (47d)$$

we define four on-shell conditions by introducing new s_{ij} $(i,j=1,2)$ as

$$s_{21} + u_2 + t_1 = 4m^2, \qquad (48a)$$

$$s_{12} + u_1 + t_2 = 4m^2, \qquad (48b)$$

$$s_{22} + u_2 + t_2 = 4m^2, \qquad (48c)$$

$$s_{11} + u_1 + t_1 = 4m^2, \qquad (48d)$$

where

$$s_{21} = s_i - 2p'_2 \cdot K, \tag{49a}$$

$$s_{12} = s_i - 2p'_1 \cdot K, \tag{49b}$$

$$s_{22} = s_f + 2p_1 \cdot K, \tag{49c}$$

$$s_{11} = s_f + 2p_2 \cdot K. \tag{49d}$$

Equations (48a)–(48d) show that there are only two independent variables in a given set of (s_{ij}, u_i, t_j) $(i,j=1,2)$. Thus, we can write

$$F_\alpha(u_1, t_1) = F_\alpha(s_{11}, t_1), \tag{50a}$$

$$F_\alpha(u_1, t_2) = F_\alpha(s_{12}, t_2), \tag{50b}$$

$$F_\alpha(u_2, t_1) = F_\alpha(s_{21}, t_1), \tag{50c}$$

$$F_\alpha(u_2, t_2) = F_\alpha(s_{22}, t_2). \tag{50d}$$

Equations (49a)–(49d) and Eqs. (50a)–(50d) show that the on-shell points (s_{ij}, t_j) $(i,j=1,2)$, at which the amplitudes $F_\alpha(u_i, t_j) = F_\alpha(s_{ij}, t_j)$ are to be evaluated, involve off-shell contributions because s_{ij} include off-shell factors. (For further discussion of this point, see the Appendix.)

Now, from the four s_{ij}, four center-of-mass momenta can be defined,

$$q^{ij}_{\text{c.m.}} = \frac{1}{2}\sqrt{s_{ij} - 4m^2}, \tag{51}$$

and four center-of-mass angles can be obtained from $q^{ij}_{\text{c.m.}}$ and t_j,

$$\cos\theta^{ij}_{\text{c.m.}} = 1 + \frac{t_j}{2(q^{ij}_{\text{c.m.}})^2}. \tag{52}$$

Therefore, $F_\alpha(s_{ij}, t_j)$ will be evaluated at a given set of $(q^{ij}_{\text{c.m.}}, \theta^{ij}_{\text{c.m.}})$,

$$F_\alpha(u_i, t_j) = F_\alpha(s_{ij}, t_j) = F_\alpha(q^{ij}_{\text{c.m.}}, \theta^{ij}_{\text{c.m.}}). \tag{53}$$

The five invariant amplitudes $F_\alpha(q^{ij}_{\text{c.m.}}, \theta^{ij}_{\text{c.m.}})$ $(\alpha = 1, 2, \ldots, 5)$ can be written as linear combinations of the five helicity amplitudes which are explicit functions of the pp phase shifts. In this work, phase shifts and mixing parameters from the Nijmegen pp partial-wave analysis PWA93 [19,20] have been used to evaluate $F_\alpha(q^{ij}_{\text{c.m.}}, \theta^{ij}_{\text{c.m.}})$.

IV. RESULTS AND DISCUSSION

We present here several results, in addition to those appearing in Ref. [1], which demonstrate the existence of significant noncoplanarity effects in $pp\gamma$. Specific calculations are illustrated in Figs. 4–12. Three different types of plots are involved in these figures: (i) The first type of plot is in terms of the standard noncoplanar curves, which are defined as the dependence of the differential cross section $d^3\sigma/d\Omega_1 d\Omega_2 d\psi_\gamma$ upon the noncoplanar angle $\bar\phi$ for a given
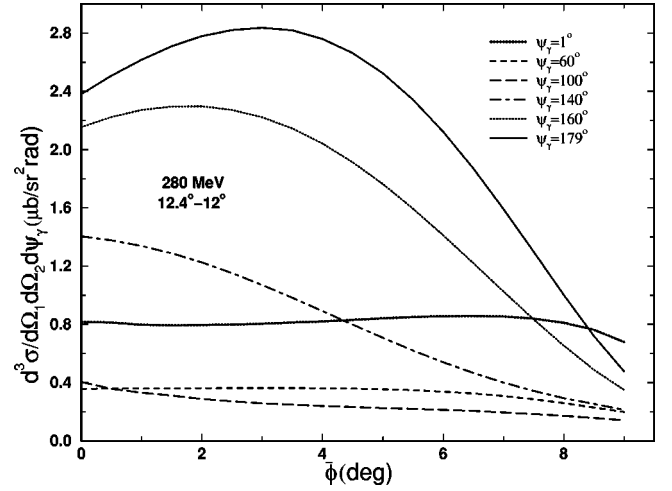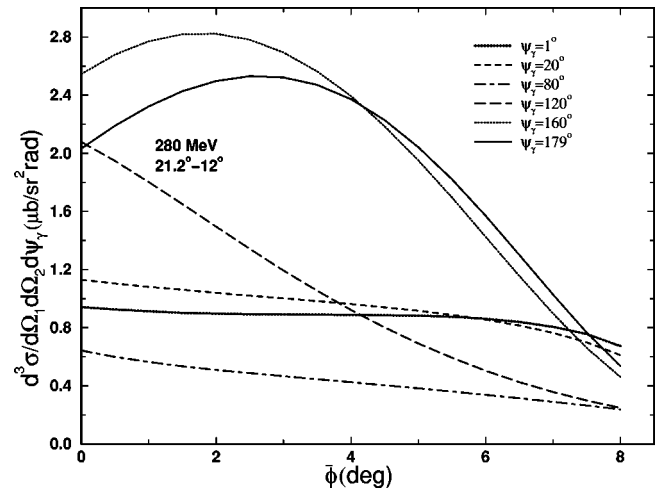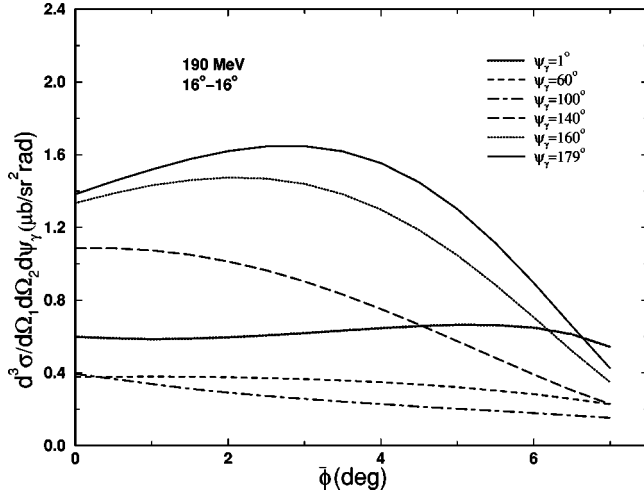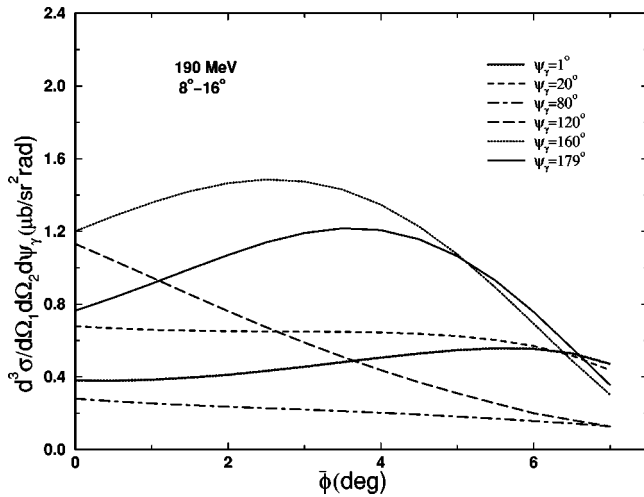

FIG. 4. Noncoplanar $pp\gamma$ cross sections as a function of the noncoplanar angle $\bar\phi$ at an incident energy of 280 MeV for the angle pair $(\bar\theta_1, \bar\theta_2) = (12.4°, 12°)$ and various ψ_γ.

photon angle ψ_γ (i.e., $d^3\sigma/d\Omega_1 d\Omega_2 d\psi_\gamma$ as a function of $\bar\phi$ for a given ψ_γ). Noncoplanarity effects can be determined from such a curve. An important application lies in estimating the angular dependent correction factor $C(\psi_\gamma)$. As shown in Eq. (5) of Ref. [1],

$$
\begin{aligned}
(d^3\sigma/d\Omega_1 d\Omega_2 d\theta_\gamma)_{exp} \\
= [C(\psi_\gamma)(d^3\sigma/d\Omega_1 d\Omega_2 d\psi_\gamma)_{exp}]_{\psi_\gamma = \theta_\gamma}.
\end{aligned} \tag{54}
$$

This factor relates the experimental noncoplanar cross section $(d^3\sigma/d\Omega_1 d\Omega_2 d\psi_\gamma)_{exp}$ at ψ_γ to an "experimental" coplanar cross section $(d^3\sigma/d\Omega_1 d\Omega_2 d\theta_\gamma)_{exp}$ at θ_γ. (ii) The second type of plot is the cross section ratio $d^3\sigma/d\Omega_1 d\Omega_2 d\psi_\gamma/(d^3\sigma/d\Omega_1 d\Omega_2 d\psi_\gamma)_{\bar\phi=0}$ as a function of ψ_γ for a given $\bar\phi$. (iii) The third type of plot is the typical

FIG. 5. Noncoplanar $pp\gamma$ cross sections as a function of the noncoplanar angle $\bar\phi$ at an incident energy of 280 MeV for the angle pair $(\bar\theta_1, \bar\theta_2) = (21.2°, 12°)$ and various ψ_γ.

FIG. 6. Noncoplanar $pp\gamma$ cross sections as a function of the noncoplanar angle $\bar{\phi}$ at an incident energy of 190 MeV for the angle pair $(\bar{\theta}_1, \bar{\theta}_2) = (16°, 16°)$ and various ψ_γ.
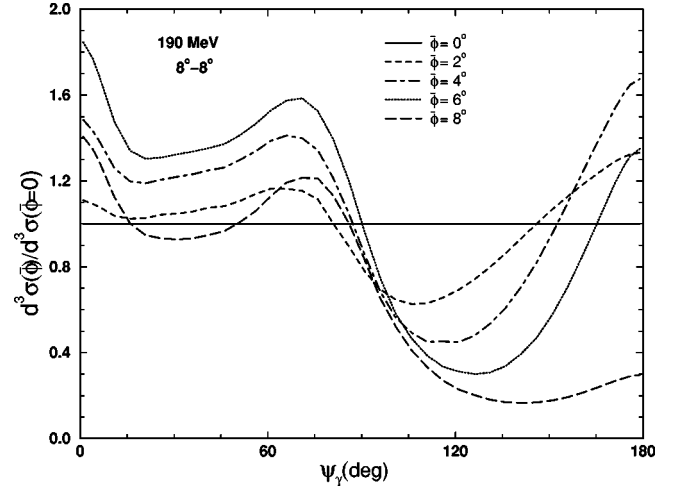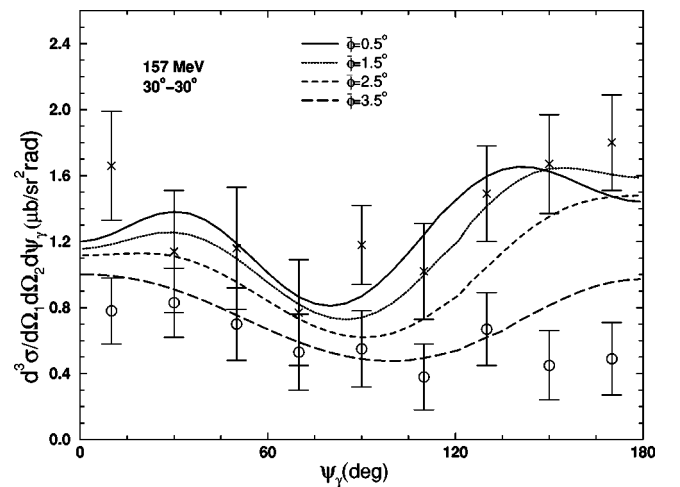

FIG. 8. Noncoplanar $pp\gamma$ cross section ratios as a function of ψ_γ at an incident energy of 190 MeV for the angle pair $(\bar{\theta}_1, \bar{\theta}_2) = (8°, 8°)$ and various $\bar{\phi}$. All curves have been normalized to the coplanar case at $\bar{\phi} = 0°$.

noncoplanar curve used in the past. It depicts the noncoplanar cross section $d^3\sigma/d\Omega_1 d\Omega_2 d\psi_\gamma$ as a function of ψ_γ for a given $\bar{\phi}$.

In Fig. 4, we present noncoplanar curves of the first type for $(\bar{\theta}_1, \bar{\theta}_2) = (12.4°, 12°)$ at an incident energy of 280 MeV, the energy of the TRIUMF experiment [31]. Six different curves corresponding to $\psi_\gamma = 1°$, 60°, 100°, 140°, 160°, and 179° are shown. The following interesting features can be observed from these six curves: (i) Noncoplanarity effects are rather insignificant for $\psi_\gamma = 1°$, 60°, and 100°. The corresponding noncoplanar curves are insensitive to the variation of $\bar{\phi}$. However, as shown in Fig. 1 of Ref. [1], noncoplanarity effects are significant in the regions $\psi_\gamma < 15°$ for $\bar{\theta}_1 = \bar{\theta}_2 = 8°$ at an incident energy of 190 Mev. This would imply that noncoplanarity effects become more significant in the regions of small ψ_γ as the scattering angle of the two

final-state protons is decreased. We also observe that cross sections are small for $\psi_\gamma = 60°$ and 100°, due to the quadrupole nature of the radiation. (ii) Cross sections vary rapidly as a function of $\bar{\phi}$ for $\psi_\gamma = 140°$, 160°, and 179°, implying that noncoplanarity effects are significant at back angles. Generally speaking, it is correct to state that noncoplanarity effects are more important for the backward scattering process than for the forward scattering process. The KVI experiment observed significant noncoplanarity effects primarily because the range of θ_γ covered in their (spherical geometry) experiment lies between 135° and 165° in the "supercluster" geometry and between 65° and 165° in the "block" geometry. It should be pointed out that the contribution from most higher-order effects (mentioned in our introduction) is significant in the regions $\psi_\gamma < 20°$ and $\psi_\gamma > 160°$. Thus, the

FIG. 7. Noncoplanar $pp\gamma$ cross sections as a function of the noncoplanar angle $\bar{\phi}$ at an incident energy of 280 MeV for the angle pair $(\bar{\theta}_1, \bar{\theta}_2) = (8°, 16°)$ and various ψ_γ.

FIG. 9. Noncoplanar $pp\gamma$ cross sections as a function of ψ_γ at an incident energy of 157 MeV for the angle pair $(\bar{\theta}_1, \bar{\theta}_2) = (30°, 30°)$ and various $\bar{\phi}$. The data for $\bar{\phi} = 1.5°$ (crosses) and for $\bar{\phi} = 3.5°$ (circles) are from the Harvard experiment (Ref. [9]).
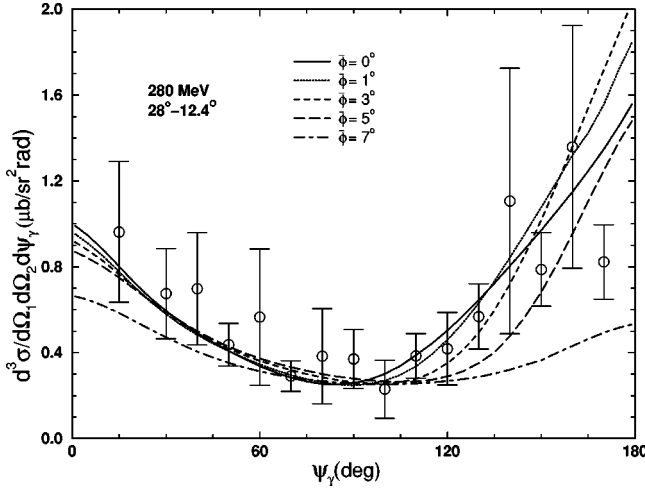
FIG. 10. Noncoplanar $pp\gamma$ cross sections as a function of ψ_γ at an incident energy of 280 MeV for the angle pair $(\bar{\theta}_1,\bar{\theta}_2)=(28°,12.4°)$ and various $\bar{\phi}$. The coplanar data are from the TRIUMF experiment (Ref. [31]).
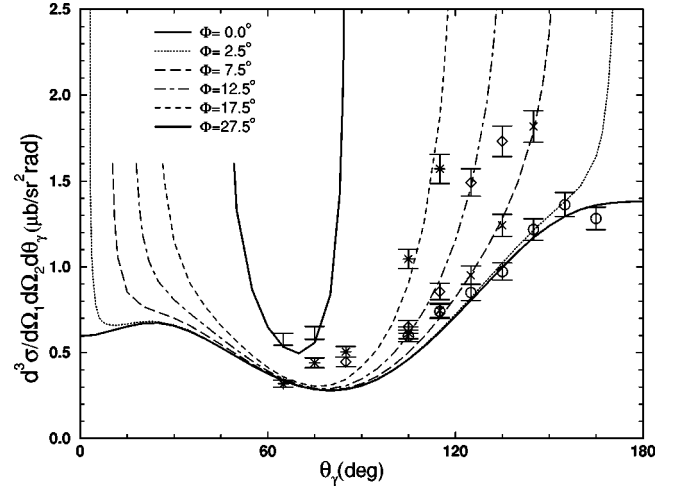

FIG. 11. Noncoplanar $pp\gamma$ cross sections $(d^3\sigma/d\Omega_1 d\Omega_2 d\theta_\gamma)$ as a function of θ_γ at an incident energy of 190 MeV for the angle pair $(\theta_1,\theta_2)=(16°,16°)$ and various Φ. The noncoplanar data [$\Phi=2.5°$ (circles), $\Phi=7.5°$ (crosses), $\Phi=12.5°$ (diamonds), $\Phi=17.5°$ (asterisks), and $\Phi=27.5°$ (dots)] are from the KVI experiment (Refs. [3,4]).

discrepancy between theory and experiment for the coplanar case in these two regions may depend upon a complex combination of effects, requiring thorough theoretical and experimental investigation to understand. (iii) Near the maximum $\bar{\phi}(=\bar{\phi}_{max})$, the six curves converge to imply similar cross sections. (iv) In the past a unique noncoplanar curve, which represents the integrated cross section (or the double differential cross section) as a function of $\bar{\phi}$, was either calculated theoretically or measured experimentally. If such a curve is used to obtain a correction factor C, then C will be a constant; that is, C will be independent of ψ_γ. However, the fact that all six curves shown in this figure differ significantly implies that noncoplanarity effects depend on ψ_γ. The correction factors $C(\psi_\gamma)$ obtained from these curves will vary with ψ_γ. Thus, the first type of plot gives a very useful picture for investigating noncoplanarity effects.

We show three more such plots in Fig. 5 [at 280 MeV for $(\bar{\theta}_1,\bar{\theta}_2)=(21.2°,12°)$], Fig. 6 [at 190 MeV for $(\bar{\theta}_1,\bar{\theta}_2)=(16°,16°)$], and Fig. 7 [at 190 MeV for $(\bar{\theta}_1,\bar{\theta}_2)=(8°,16°)$]. Again, very similar features as are observed in Fig. 4 can be found in these figures. This strongly suggests that such features are more or less universal.

In Fig. 8, we show a second type of plot at 190 MeV for $\bar{\theta}_1=\bar{\theta}_2=8°$ and $\bar{\phi}=0°$, 2°, 4°, 6°, and 8°. The curves in this figure show a complex noncoplanar behavior, because of the small proton angles. This complication is reflected in the plot of the first type shown in Fig. 1 of Ref. [1] for the identical case. Such a complexity would be less prominent in an analogous plot for 157 MeV and $\bar{\theta}_1=\bar{\theta}_2=30°$, because for larger proton angles the cross section decreases more monotonically with increasing $\bar{\phi}$ for almost all ψ_γ.

The above comment is also illustrated in Fig. 9, where we show the third type of plot at 157 MeV for $\bar{\theta}_1=\bar{\theta}_2=30°$ and $\bar{\phi}=0.5°$, 1.5°, 2.5°, and 3.5°. At this energy and for these large proton angles, noncoplanarity effects are not compli-

cated. We include data from the Harvard experiment [9] for comparison with the theoretical curves. One observes that, for a given $\psi_\gamma(\lesssim 140°)$, the cross section decreases monotonically with increasing $\bar{\phi}$. The theoretical curves describe well the noncoplanar data for the two ranges of $\bar{\phi}$ shown. Such plots also demonstrate that all curves (for the cross section $d^3\sigma/d\Omega_1 d\Omega_2 d\psi_\gamma$) are free of kinematic singularity.

In Fig. 10, we present a similar plot at 280 MeV for $(\bar{\theta}_1,\bar{\theta}_2)=(28°,12.4°)$ and $\bar{\phi}=0°,1°$, 3°, 5°, and 7°. These noncoplanar curves indicate that noncoplanarity effects are much more significant in the region of $\psi_\gamma>90°$ than in the region of $\psi_\gamma<90°$. We include the coplanar data from the TRIUMF experiment [31] for comparison. The figure confirms that noncoplanar effects could play a role in understanding the back angle data.

In Fig. 11, we compare our calculated noncoplanar cross sections with the KVI data [3,4] at 190 MeV for the angles $(\theta_1,\theta_2)=(16°,16°)$ in the spherical coordinate system. Using the spherical coordinate system [32], the KVI experiment measured the noncoplanar cross section of the form $d^3\sigma/d\Omega_1 d\Omega_2 d\theta_\gamma$. Here, we plot the cross section as a function of θ_γ for the noncoplanarity angles $\Phi=0°$, 2.5°, 7.5°, 12.5°, 17.5°, and 27.5°. (See Ref. [32] for the definition of Φ. This noncoplanarity angle Φ, defined in the spherical coordinate system [32], is different from our $\bar{\phi}$, defined in the Harvard coordinate system.) The maximum noncoplanarity angle in this case is $\Phi_{max}=29.0°$. Due to the phase-space factor, the range of θ_γ decreases as Φ increases, and the cross section diverges at both ends of the range of θ_γ. The experimental data for $\Phi=2.5°$ were considered to be coplanar [2–4] and compared as such with theoretical calculations. Note, however, that our calculations show that the difference between the cross sections for $\Phi=0°$ (coplanar) and $\Phi=2.5°$ (noncoplanar) is significant for $\theta_\gamma>145°$. In general, the agreement between our calculations and the experi-
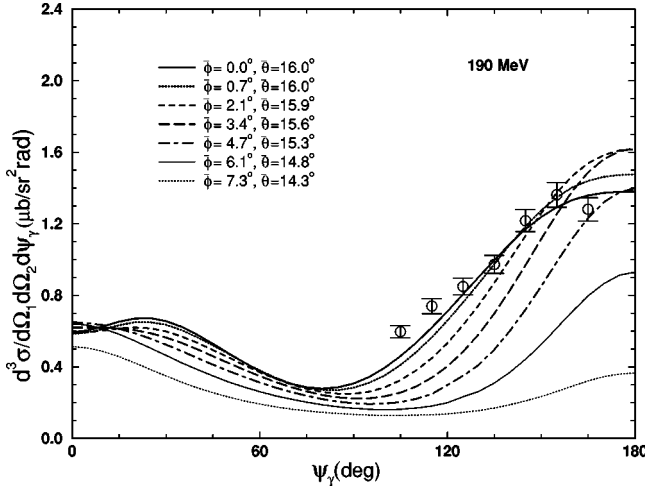
FIG. 12. Noncoplanar $pp\gamma$ cross sections as a function of ψ_γ at an incident energy of 190 MeV for various $(\bar{\theta}_1, \bar{\theta}_2)$ and various $\bar{\phi}$. The data (for $\Phi=2.5°$) are from the KVI experiment (Refs. [2,3]).

mental data is good, especially for the data with small non-coplanarity angles (less than 12.5°).

Finally, in Fig. 12, we show the corresponding cross sections at 190 MeV in Harvard coordinates. For fixed $\theta_1=\theta_2=16°$ and for varying noncoplanarity angles $\Phi=2.5°$, $7.5°$, $12.5°$, $17.5°$, $22.5°$, and $27.5°$ in the spherical coordinate system, the corresponding polar and noncoplanarity angles in the Harvard coordinate system are given by $(\overline{\theta_1}=\overline{\theta_2},\bar{\phi})$ $=(16.0°,0.7°)$, $(15.9°,2.1°)$, $(15.6°,3.4°)$, $(15.3°,4.8°)$, $(14.8°,6.1°)$, and $(14.3°,7.3°)$, respectively. The maximum noncoplanarity angle is $\bar{\phi}_{max}=7.69°$. The "coplanar" KVI data are added for comparison. Figure 12 again demonstrates that noncoplanarity effects are indeed much more significant in the region of $\psi_\gamma>90°$ than in the region of $\psi_\gamma<90°$.

In conclusion, we find that noncoplanar effects in proton-proton bremsstrahlung are non-negligible. Therefore, noncoplanarity should be properly included in any analysis of experimental $pp\gamma$ data. Moreover, special care should be exercised in attempting to draw conclusions from a comparison of experimental data with purely coplanar calculations.

ACKNOWLEDGMENTS

APPENDIX: SOFT-PHOTON APPROXIMATION

The soft-photon approximation is based upon a fundamental theorem, known as the soft-photon theorem, first derived by Low [21] in 1958. If one writes a bremsstrahlung amplitude M_μ as an expansion in powers of the photon energy K (the soft-photon expansion),

$$M_\mu = \frac{A_\mu}{K} + B_\mu + C_\mu K + \cdots, \tag{A1}$$

where

$$A_\mu = \lim_{K \to 0}(KM_\mu),$$

$$B_\mu = \lim_{K \to 0}\frac{\partial}{\partial K}(KM_\mu)_{x_i},$$

$$C_\mu = \frac{1}{2}\lim_{K \to 0}\frac{\partial^2}{\partial K^2}(KM_\mu)_{x_i}, \tag{A2}$$

then the theorem states that the first two coefficients, A_μ and B_μ [or the first two terms of the expansion $(A_\mu/K+B_\mu)$] may be calculated exactly in terms of the corresponding elastic scattering amplitude and electromagnetic constants of the participating particles. In Eq. (A2), the x_i refer to a set of independent variables which are held constant in carrying out the partial differentiation. Thus, the soft-photon amplitude is defined to be

$$M_\mu^{SPA} = \frac{A_\mu}{K} + B_\mu. \tag{A3}$$

In terms of this amplitude, the soft-photon cross section has the form

$$\sigma^{SPA} = \frac{\sigma_{-1}}{K} + \sigma_0 + \bar{\sigma}_1 K. \tag{A4}$$

Historically, Low defined the soft-photon theorem directly in terms of the bremsstrahlung cross section σ. In this case, the soft-photon expansion gives

$$\sigma = \frac{\sigma_{-1}}{K} + \sigma_0 + \sigma_1 K + \cdots, \tag{A5}$$

where

$$\sigma_{-1} = \lim_{K \to 0}(K\sigma),$$

$$\sigma_0 = \lim_{K \to 0}\frac{\partial}{\partial K}(K\sigma)_{x_i},$$

$$\sigma_1 = \frac{1}{2}\lim_{K \to 0}\frac{\partial^2}{\partial K^2}(K\sigma)_{x_i}, \tag{A6}$$

and the theorem states that the first two terms (σ_{-1}/K and σ_0) of this expansion may be evaluated exactly in terms of the corresponding elastic scattering amplitude and the electromagnetic constants of the participating particles. The soft-photon cross section can be defined as

$$\sigma_L^{SPA} = \frac{\sigma_{-1}}{K} + \sigma_0 . \tag{A7}$$

Note that because of the extra term $\bar{\sigma}_1 K$ [which is not identical to $\sigma_1 K$ in Eq. (A5)] in Eq. (A4), σ^{SPA} is not equal to σ_L^{SPA}.

Let us first discuss two different interpretations of the soft-photon expansion and theorem. (i) Rigorously speaking [22], the expansion given by Eq. (A1) [or Eq. (A5)] implies the following conditions:

(A) K must be an independent variable and it has a range including the point at $K=0$.

(B) The expansion of M_μ (or σ) must be carried out not only for those dynamical terms (or factors) which are explicit functions of K but also for those dependent kinematic variables which are implicit functions of K. In other words, the kinematics and dynamics of the bremsstrahlung process should be expanded consistently and completely.

(C) The coefficients $A_\mu, B_\mu, \quad C_\mu, \ldots$, etc. (or $\sigma_{-1}, \sigma_0, \sigma_1, \ldots$, etc.) exist and they are independent of K. They are to be evaluated at a unique on-shell point, (s,t) or (u,t). Here, t and u are defined by Eq. (34).

These three conditions assure that the soft-photon amplitude M_μ^{SPA} (or the soft-photon cross section σ_L^{SPA}) physically exists and it is independent of the off-mass-shell (or off-energy-shell) effects. When σ_L^{SPA} is plotted as a function of K, Eq. (A7) yields a family of hyperbolas characterized by two K-independent constants σ_{-1} and σ_0.

This rigorous interpretation of the soft-photon expansion and theorem does not always apply to all types of cross section. As an example, let us choose the set $(\theta_1, \phi_1, \theta_2, \phi_2, \theta_\gamma)$ to be independent variables and express the cross section in the form $d^3\sigma/d\Omega_1 d\Omega_2 d\theta_\gamma$. This is a common choice for those experiments which use the Harvard geometry, and this type of cross section is classified as the H-type cross section [22]. In this case, the dependent variables are p_1', p_2', ϕ_γ, and K. Since K is not an independent variable and the range of K does not include the point at $K=0$, we cannot let K approach zero arbitrarily (or simply set K equal to zero). Thus, "the limit K tends to zero" does not physically exist under the restriction of energy-momentum conservation. In fact (as pointed out in Ref. [22]), because the condition $p_1^\mu + p_2^\mu - p_1'^\mu - p_2'^\mu - K^\mu \neq 0$ at $K=0$ would imply that $\delta^4(p_1 + p_2 - p_1' - p_2' - K) = 0$, the cross section $d^3\sigma/d\Omega_1 d\Omega_2 d\theta_\gamma$ must vanish at $K=0$. We therefore conclude that the soft-photon expansion given by Eq. (A5) does not physically exist for the cross section $d^3\sigma/d\Omega_1 d\Omega_2 d\theta_\gamma$, and hence the soft-photon theorem defined in terms of Eq. (A5) cannot be rigorously derived for this type of cross section.

The soft-photon expansion exists only for the R-type cross section. For example, if we choose the set $(\theta_1, \phi_1, \theta_\gamma, \phi_\gamma, K)$ to be the independent variables and express the cross section in the form $d^3\sigma/d\Omega_1 d\Omega_\gamma dK$, then the above three conditions are satisfied and the soft-photon theorem can be rigorously derived for the cross section $d^3\sigma/d\Omega_1 d\Omega_\gamma dK$. We refer to Ref. [22] for detailed discussion.

(ii) The second interpretation applies to both H-type and R-type cross sections, though it is absolutely required in the case of the H-type cross section. In this second interpretation, the above three conditions are modified as follows:

(A') K may or may not be an independent variable and its range may or may not include the point at $K=0$.

(B') The expansion of M_μ (or σ) applies only to those terms which are explicit functions of K.

(C') The coefficients $A_\mu, B_\mu, C_\mu, \ldots$, (or $\sigma_{-1}, \sigma_0, \sigma_1, \ldots$) may still be functions of K. They can be evaluated at different on-shell points.

In this second interpretation, the statement "the limit K tends to zero" in Eqs. (A2) and (A6) means that we simply set those terms which depend explicitly on K to be zero. An important aspect of this interpretation is that it allows a choice of different on-shell points, at which A_μ and B_μ (or σ_{-1} and σ_0) can be evaluated. This is because the soft-photon theorem, under the second interpretation, does not specify how these on-shell points are to be selected. Thus, various soft-photon amplitudes (or cross sections) which are evaluated at different on-shell points can be constructed. But the difference between any two soft-photon amplitudes is always $O(K)$. For a detailed discussion and examples, see Ref. [23]. An example of choosing different on-shell points for the $TuTts$ amplitude is discussed in Sec. III of this work [see Eqs. (45)–(50d)].

In general, on-shell points can be chosen from $u_{\bar{\alpha},\bar{\beta}}^-$, $t_{\bar{\alpha}',\bar{\beta}'}^-$, and $s_{\bar{\alpha}'',\bar{\beta}''}^-$. Here $u_{\bar{\alpha},\bar{\beta}}^-$, and $t_{\bar{\alpha}',\bar{\beta}'}^-$ are defined by Eqs. (45) and (46), respectively (but with the new constraints $\bar{\alpha} + \bar{\beta} \neq 0$, $\bar{\alpha} \geq 0$, $\bar{\beta} \geq 0$ and $\bar{\alpha}' + \bar{\beta}' \neq 0$, $\bar{\alpha}' \geq 0$, $\bar{\beta}' \geq 0$), and $s_{\bar{\alpha}'',\bar{\beta}''}^-$ is a linear combination of s_i and s_f,

$$s_{\bar{\alpha}'',\bar{\beta}''}^- = \frac{\bar{\alpha}'' s_i + \bar{\beta}'' s_f}{\bar{\alpha}'' + \bar{\beta}''}, \quad \bar{\alpha}'' \geq 0, \quad \bar{\beta}'' \geq 0, \quad \bar{\alpha}'' + \bar{\beta}'' \neq 0. \tag{A8}$$

Depending upon the choice of the on-shell points, at which the soft-photon amplitude M_μ^{SPA} is to be evaluated, we can construct two distinct classes of soft-photon amplitudes: $M_\mu^{(1)}(u,t)$ and $M_\mu^{(2)}(s,t)$. These two classes of amplitudes have been investigated [24] and the most important results can be summarized as follows:

(1) The (u,t) class $M_\mu^{(1)}(u,t)$: The on-shell points for this class of soft-photon amplitudes can be chosen from $(u_{\bar{\alpha},\bar{\beta}}^-, t_{\bar{\alpha}',\bar{\beta}'}^-)$. That is, an infinite number of on-shell points can be used. This theoretical ambiguity cannot be avoided if we apply *only* the soft-photon theorem (under the second interpretation) to construct soft-photon amplitudes [i.e., the $M_\mu^{(1)}(u,t)$ amplitudes in this case]. However, the soft-photon theorem *alone* cannot provide a correct bremsstrahlung amplitude for a given bremsstrahlung process. Other theoretical constraints are also required. In fact, these additional theoretical constraints for any bremsstrahlung process can be used to find the right class of amplitude [$M_\mu^{(1)}(u,t)$ or $M_\mu^{(2)}(s,t)$] for the process and to determine specific on-shell points at which to evaluate the constructed soft-photon amplitude. Therefore, the theoretical ambiguity can be removed. Let us use the $pp\gamma$ process as an example to illustrate this point. For this process, we have to impose at least the following additional constraints: (1a) The constructed soft-

photon amplitude M_μ must obey the Pauli principle [15]. (1b) The constructed soft-photon amplitude should be relativistic and its internal amplitude M_μ^I must satisfy the analyticity condition [25]. (1c) The amplitude M_μ should reduce to the corresponding special amplitude $\bar{M}_\mu$ at the tree-level approximation [24]. In our case, in order to be consistent with the meson theory of the NN interaction, $\bar{M}_\mu$ is the bremsstrahlung amplitude derived from the one-boson-exchange (OBE) diagrams. The constraint (1a) implies that all amplitudes $M_\mu^{(2)}(s,t)$, except for Low's original amplitude, cannot be used to describe the $pp\gamma$ process because these amplitudes violate the Pauli principle. The constraint (1b) is a fundamental requirement and it should not be compromised because of the soft-photon approximation. Those terms which violate the analyticity condition do not belong to the internal amplitude. It is the constraint (1c) which demands that a valid soft-photon amplitude should be in the (u,t) class. Guided by all three additional constraints, a soft-photon amplitude has been rigorously derived in Ref. [15]. This amplitude is the two-u–two-t special amplitude $M_\mu^{TuTts}(u_1,u_2,t_1,t_2)$ used in this work, Eqs. (40)–(44). It should be pointed out that M_μ^{TuTts} depends on the elastic pp amplitude $[F_\alpha(u_i,t_j)\ (i,j=1,2)]$ evaluated at four special on-shell points (u_1,t_1), (u_1,t_2), (u_2,t_1), and (u_2,t_2). Thus, the constraint (1c) rules out the possibility of evaluating F_α at any combination of $(u_{\bar{\alpha},\bar{\beta}})$ and any combination of $(t_{\bar{\alpha}',\bar{\beta}'})$.

Although the amplitude M_μ^{TuTts} has already been discussed in Sec. III B, the following four remarks will help us to understand some important features of this amplitude:

(i) We should emphasize that

$$F_\alpha(u_2,t_1)=F_\alpha(s_{21},t_1)\neq F_\alpha(s_i,t_1), \qquad \text{(A9a)}$$

$$F_\alpha(u_1,t_2)=F_\alpha(s_{12},t_2)\neq F_\alpha(s_i,t_2), \qquad \text{(A9b)}$$

$$F_\alpha(u_2,t_2)=F_\alpha(s_{22},t_2)\neq F_\alpha(s_f,t_2), \qquad \text{(A9c)}$$

$$F_\alpha(u_1,t_1)=F_\alpha(s_{11},t_1)\neq F_\alpha(s_f,t_1). \qquad \text{(A9d)}$$

As explained in Sec. III B, the four on-shell conditions given by Eqs. (48a)–(48d) allow us to write the four relations given by Eqs. (50a)–(50d). Equations (47a)–(47d) can be used to explain the four inequalities given by Eqs. (A9a)–(A9d), respectively. For example, let us use Equation (47a) to explain Eq. (A9a). Equation (47a) involves four kinematical variables: three Mandelstam variables (s_i,u_2,t_1) and an off-shell factor $2p_2'\cdot K$, which is related to the square of the invariant mass of the off-mass-shell p_2' leg $[(p_2'+K)^2=m^2+2p_2'\cdot K]$ on which the photon emission occurs. In other words, Eq. (47a) is not an on-shell condition because there are three independent variables in this equation. One cannot simply ignore the off-shell factor $2p_2'\cdot K$ and set $F_\alpha(u_2,t_1)$ equal to $F_\alpha(s_i,t_1)$. Thus, while the condition given by Eq. (48a) permits us to evaluate the amplitude $F_\alpha(u_2,t_1)$ at the on-shell point (s_{21},t_1), the condition given by Eq. (47a) forbids us to evaluate these amplitudes at the on-shell points (s_i,t_1).

(ii) We choose the set $(\bar{\theta}_1,\bar{\phi}_1,\bar{\theta}_2,\bar{\phi}_2,\psi_\gamma)$ to be the independent variables and calculate the cross section of the form $d^3\sigma/d\Omega_1 d\Omega_2 d\psi_\gamma$. The dependent variables are p_1', p_2', K, and $\bar{\phi}_\gamma$. Since K is not an independent variable, we cannot let K approach zero arbitrarily. Moreover, the range of K does not include the point $K=0$, i.e. $0\neq K_{min}\leqslant K\leqslant K_{max}$. Therefore, all off-shell factors ($2p_1\cdot K$, $2p_2\cdot K$, $2p_1'\cdot K$, and $2p_2'\cdot K$) must be greater than zero and we have

$$s_{21}=s_i-2p_2'\cdot K<s_i, \qquad \text{(A10a)}$$

$$s_{12}=s_i-2p_1'\cdot K<s_i, \qquad \text{(A10b)}$$

$$s_{22}=s_f+2p_1\cdot K>s_f, \qquad \text{(A10c)}$$

$$s_{11}=s_f+2p_2\cdot K>s_f. \qquad \text{(A10d)}$$

Equations (A10a)–(A10d) imply that

$$s_f<(s_{22},s_{21},s_{12},s_{11})<s_i. \qquad \text{(A11)}$$

These results lead to the following interpretation. Equations (A10a), (50a), and (A9a) show that the off-shell factor $-2p_2'\cdot K$ reduces s_i to s_{21} and shifts the on-shell point from (s_i,t_1) to (s_{21},t_1) for the amplitude $F_\alpha(u_2,t_1)=F_\alpha(s_{21},t_1)$. Equation (A10b), (50b), and (A9b) show that the off-shell factor $-2p_1'\cdot K$ reduces s_i to s_{12} and shifts the on-shell point from (s_i,t_2) to (s_{12},t_2) for the amplitude $F_\alpha(u_1,t_2)=F_\alpha(s_{12},t_2)$. Equation (A10c), (50c), and (A9c) show that the off-shell factor $2p_1'\cdot K$ boosts s_f to s_{22} and shifts the on-shell point from (s_f,t_2) to (s_{22},t_2) for the amplitude $F_\alpha(u_2,t_2)=F_\alpha(s_{22},t_2)$. Equation (A10d), (50d), and (A9d) show that the off-shell factor $2p_2'\cdot K$ boosts s_f to s_{11} and shifts the on-shell point from (s_f,t_1) to (s_{11},t_1) for the amplitude $F_\alpha(u_1,t_1)=F_\alpha(s_{11},t_1)$. Now s_{ij} can be used to define four kinetic energies of the proton in the c.m. system. We find

$$T_{\text{c.m.}}^{ij}=\sqrt{s_{ij}}/2-m. \qquad \text{(A12)}$$

Similarly, s_i and s_f can also be used to define two kinetic energies of the proton in the c.m. system. We obtain

$$T_{\text{c.m.}}^{(i)}=\sqrt{s_i}/2-m, \qquad \text{(A13)}$$

$$T_{\text{c.m.}}^{(f)}=\sqrt{s_f}/2-m. \qquad \text{(A14)}$$

From Eq. (A11), we can show that

$$T_{\text{c.m.}}^{(f)}<T_{\text{c.m.}}^{ij}<T_{\text{c.m.}}^{(i)}. \qquad \text{(A15)}$$

Equation (A15) explains why the kinetic energies $T_{\text{c.m.}}^{ij}$ used in the $TuTts$ amplitude never reach $T_{\text{c.m.}}^{(i)}$ or $T_{\text{c.m.}}^{(f)}$. For example, at 190 MeV, $T_{\text{c.m.}}^{(f)}$ may reach an energy as low as 10 MeV for some cases, but Eq. (A15) shows that $T_{\text{c.m.}}^{ij}$ will always be greater than 10 MeV. Again, this is because $T_{\text{c.m.}}^{ij}$ (or s_{ij}) involve off-shell contributions.

(iii) All on-shell points, (s_{ij},t_j) [or $(q_{\text{c.m.}}^{ij},\theta_{\text{c.m.}}^{ij})$ defined by Eqs. (51) and (52)], can be defined in the whole phase

space. In other words, the angles $\theta_{c.m.}^{ij}$ can be physically defined in the whole phase space without any problem. On the other hand, if we choose the on-shell points to be (s_i,t_1), (s_i,t_2), (s_f,t_1), and (s_f,t_2), then these points will have a phase-space problem [26], which was first discussed in Ref. [27]. The reason is as follows [27]. From s_i and s_f, two c.m. momenta can be defined,

$$q_{c.m.}^{(x)} = \frac{1}{2}\sqrt{s_x - 4m^2} \quad (x=i,f), \tag{A16}$$

and four c.m. scattering angles $\theta_{c.m.}^{xj}$ can be determined from $q_{c.m.}^{(x)}$ and t_j $(j=1,2)$,

$$\cos\theta_{c.m.}^{xj} = 1 + t_j/[2(q_{c.m.}^{(x)})^2]. \tag{A17}$$

This is the so-called two-energy–four-angle approximation. The phase-space problem associated with this approximation is that not all $\theta_{c.m.}^{ij}$ angles can be physically defined in the whole phase space. As discussed in remark (i) above, this problem arises because the on-shell points used in this approximation have ignored all off-shell factors shown in Eqs. (47a)–(47d). Furthermore, the two-s–two-t special ($TsTts$) amplitude violates the Pauli principle.

(iv) The $TuTts$ amplitude M_μ^{TuTts} is different from Low's original amplitude [21] for several reasons. A major difference between these two amplitudes is that they use very different on-shell conditions. The $TuTts$ amplitude uses four on-shell conditions given by Eqs. (48a)–(48d) and evaluates the pp amplitude F_α at four different on-shell points (s_{ij},t_j) $(i,j=1,2)$, while Low's amplitude utilizes a single on-shell condition,

$$\bar{s} + \bar{t} + \bar{u} = 4m^2, \tag{A18}$$

where $\bar{s}=(s_i+s_f)/2$, $\bar{t}=(t_1+t_2)/2$, and $\bar{u}=(u_1+u_2)/2$, and evaluates F_α at one on-shell point $(\bar{s},\bar{t})$. If we add the four Eqs. (47a)–(47d) together, we obtain

$$\bar{s} + \bar{t} + \bar{u} = 4m^2 + (p_1'\cdot K + p_2'\cdot K - p_1\cdot K - p_2\cdot K)/2. \tag{A19}$$

Because of energy-momentum conservation and $K_\mu K^\mu = 0$, the term involving the four off-shell factors will cancel precisely and Eq. (A19) reduces to Eq. (A18). In other words, the on-shell condition given by Eq. (A18) does not include any off-shell factors. This is quite different from the on-shell conditions given by Eqs. (48a)–(48d) which include off-shell factors through the use of the new s_{ij}. In short, the four on-shell points (s_{ij},t_j) used in the $TuTts$ amplitude take into account all off-shell factors, but the single on-shell point $(\bar{s},\bar{t})$ used in Low's amplitude is independent of off-shell factors.

Another amplitude $M_{2\mu}^{TuTts}$ given by Eq. (49) of Ref. [15] was used in Ref. [16] for $pp\gamma$ calculations. *Both M_μ^{TuTts} and $M_{2\mu}^{TuTts}$ are relativistic, gauge invariant, and consistent with the soft-photon theorem*, except that M_μ^{TuTts} obeys the Pauli principle while $M_{2\mu}^{TuTts}$ violates the Pauli principle at order

$O(K)$. We emphasize that the violation is not at $O(K/K)$ as stated in Ref. [26]; see Refs. [15,25]. Because the soft-photon approximation is specified only to $O(K)$ [i.e., violations at $O(K)$ are acceptable], the two amplitudes predict very similar results [25]. Our investigations reveal that $pp\gamma$ cross section data from low energies to energies near the pion-production threshold can be consistently described by these two amplitudes, even for those kinematic conditions where the conventional Low amplitude disagrees with experimental data or potential model calculations.

(2) The (s,t) class $M_\mu^{(2)}(s,t)$: The on-shell points for this class of soft-photon amplitudes can be chosen from $(s_{\bar{\alpha}'',\bar{\beta}''}, t_{\bar{\alpha}',\bar{\beta}'})$. Again, the fact that the soft-photon theorem allows one to choose the on-shell points arbitrarily is a theoretical ambiguity. However, as we have previously mentioned in (1) above [for the (u,t) class $M_\mu^{(1)}(u,t)$], there are other additional theoretical constraints which can be imposed in order to construct a valid $M_\mu^{(2)}(s,t)$ amplitude for a given bremsstrahlung process. This theoretical ambiguity can be removed if specific on-shell points are specified by the imposed constraints. The constraint (1c) mentioned in (1) is one such constraint. For radiative resonance scattering processes, the constraint (1c) requires that a valid amplitude should be in the (s,t) class; i.e., $M_\mu = M_\mu^{(2)}(s,t)$ and $\bar{M}_\mu = \bar{M}_\mu^{(2)}(s,t)$. This constraint can also specify certain on-shell points for the amplitude $M_\mu^{(2)}(s,t)$. Taking the $\pi^+ p\gamma$ process near the Δ^{++} resonance as an example, $\bar{M}_\mu^{(2)}(s,t)$ is the amplitude given by Eq. (54) of Ref. [28], which is derived from the Feynman diagrams shown in Fig. 2 of Ref. [28]. Reference [28] demonstrates how a general two-s–two-t special ($TsTts$) [or the two-energy–two-angle special (TETAS)] amplitude [Eq. (75) of Ref. [28]] can be constructed from $\bar{M}_\mu^{(2)}(s,t)$. {See also Refs. [24,27] for a further discussion regarding the $TsTts$ (or TETAS) amplitude.} This $TsTts$ amplitude depends upon the elastic $\pi^+ p$ amplitude evaluated at four specific on-shell points [(s_i,t_1), (s_i,t_2), (s_f,t_1), and (s_f,t_2)]. Thus, the constraint (1c) rules out the possibility of evaluating the elastic $\pi^+ p$ amplitude at arbitrary combinations of $(s_{\bar{\alpha}'',\bar{\beta}''})$ and $(t_{\bar{\alpha}',\bar{\beta}'})$. Hence the theoretical ambiguity can be removed.

The $(TsTts)$ amplitudes, which represent a class of amplitudes evaluated at $(s_i,s_f:t_1,t_2)$, were found to be optimal for processes involving strong s-channel resonance effects. Several practical versions of the $TsTts$ amplitude can be defined and two well-known versions have already been investigated. They are the two-energy–four-angle special (TEFAS) amplitudes and the TETAS amplitudes [27]. Because the center-of-mass angle $\Theta_{c.m.}$ cannot be defined for some kinematical points involving (s_f,t_1) and (s_f,t_2), the TEFAS amplitudes cannot be used for those points. This is the so-called phase-space problem. To circumvent this problem, the TETAS amplitudes were introduced in Ref. [27]. The TETAS amplitudes, which are free of the phase-space problem, have been shown to be the most successful in describing bremsstrahlung processes near a resonance.

Because $TuTts$ and TETAS amplitudes effectively describe different bremsstrahlung processes, the theoretical constraints to be imposed upon them can differ. For example, the amplitudes for the $pp\gamma$ process must obey the Pauli principle. Since the $TsTts$ amplitudes do not obey the Pauli prin-

ciple, the $TuTts$ amplitudes given by Eq. (40) should be used to describe the $pp\gamma$ process. On the other hand, in order to describe a bremsstrahlung process associated with a significant resonance, a valid amplitude must predict the correct (energy) position and width of the resonant peak, as observed in the bremsstrahlung spectrum. Using Eqs. (24) and (25) of Ref. [23], this criterion was investigated thoroughly [29]. Processes like $\pi^+ p\gamma$ [28] and $p^{12}C\gamma$ [29] in the region of a resonance can only be well described by amplitudes which are evaluated at s_i and s_f; the TETAS amplitudes were demonstrated to provide an excellent description of those processes. Equations (24) and (25) of Ref. [23] can also be applied to explain why the $TuTts$ amplitudes should not be used to describe the $\pi^+ p\gamma$ and $p^{12}C\gamma$ processes. The conventional Low amplitude fails to describe the $\pi^\pm p\gamma$ and $p^{12}C\gamma$ data in the vicinity of a resonance; in particular, it predicts incorrectly the position and width of the resonance peaks observed in the $p^{12}C\gamma$ spectrum [29].

Historically, the idea of using the two-energy–one-angle (TEOA) amplitudes to describe bremsstrahlung processes in a resonance region was first proposed by Feshbach and Yennie [30]. They realized that such amplitudes should be evaluated at two special energies: the initial energy (s_i) and the final energy (s_f), but not any linear combination of s_i and s_f. All TETAS and the special TEOA amplitudes meet this requirement (the TEFAS amplitudes also satisfy this requirement except that they have the phase-space problems). On the other hand, the conventional Low amplitude, which is typically a one-energy–one-angle amplitude, cannot be used to describe any bremsstrahlung process in the vicinity of a resonance. This is because Low's amplitude is evaluated at $\bar{s} = \frac{1}{2}(s_i + s_f)$ and $\bar{t} = \frac{1}{2}(t_1 + t_2)$. The expression for $\bar{s}$ (a linear combination of s_i and s_f),

$$\bar{s} = \frac{1}{2}(s_i + s_f) = \frac{\alpha s_i + \beta s_f}{\alpha + \beta}, \tag{A20}$$

implies that $\alpha = \beta = 1$. Substituting $\alpha = \beta = 1$ into Eqs. (24) and (25) of Ref. [23] gives $K_\gamma = 2K_0$ and $\Gamma_\gamma = 2N\Gamma_{el}$, which disagree with the observed experimental values,

$$K_\gamma \simeq K_0,$$

$$\Gamma_\gamma \simeq N\Gamma_{el} \tag{A21}$$

for the $p^{12}C\gamma$ case [29].

Feshbach and Yennie were able to derive a nonrelativistic version of the TEOA amplitude, known as the Feshbach-Yennie approximation (FYA). However, their attempt to construct a relativistic version of the TEOA amplitude was not successful. Since the amplitude involves a noncovariant term with a factor $\delta_{\mu 0}K_0^{-1}$ [see Eqs. (51a)–(50c) of Ref. [30]], the cross section calculated in the lab system and the C.M. system would yield quite different results. A relativistic version of the special TEOA amplitude (or the relativistic FYA) was discussed in Ref. [27]. The TETAS amplitude, which satisfies all theoretical constraints, can be considered as the generalized Feshbach-Yennie approximation.

In short, the $TuTts$ amplitudes are optimal for bremsstrahlung processes involving strong u-channel exchange effects while the TETAS amplitudes are optimal for those involving strong s-channel resonance effects. As for those processes which do not involve either strong u-channel exchange effects or strong s-channel resonance effects, the $TuTts$ amplitude, the TETAS amplitude, and Low's amplitude would yield similar results.

---

[1] Yi Li, M. K. Liou, R. Timmermans, and B. F. Gibson, Phys. Rev. C **58**, R1880 (1998).

[2] H. Huisman *et al.*, Phys. Rev. Lett. **83**, 4017 (1999).

[3] H. Huisman, Ph.D. thesis, University of Groningen, 1999; addendum to the thesis, KVI Internal Report KVI-216i.

[4] H. Huisman *et al.*, Phys. Lett. B **476**, 9 (2000).

[5] H. Huisman and N. Kalantar-Nayestanaki, Phys. Rev. C **64**, 029801 (2001).

[6] Yi Li, M. K. Liou, R. G. E. Timmermans, and B. F. Gibson, Phys. Rev. C **64**, 029802 (2001).

[7] M. L. Halbert, *Proceedings of the Gull Lake Symposium on the Two-Body Force in Nuclei* (Plenum, New York, 1972).

[8] K. W. Rothe, P. F. M. Koehler, and E. H. Thorndike, Phys. Rev. **157**, 1247 (1967).

[9] B. Gottschalk, W. J. Shlaer, and K. H. Wang, Nucl. Phys. **A94**, 491 (1967).

[10] M. K. Liou and M. I. Sobel, Ann. Phys. (N.Y.) **72**, 323 (1972).

[11] J. V. Jovanovich, L. G. Greeniaus, J. McKeown, T. W. Millar, D. G. Peterson, W. F. Prickett, K. F. Suen, and J. C. Thompson, Phys. Rev. Lett. **26**, 277 (1971); C. A. Smith, J. V. Jovanovich, and L. G. Greeniaus, Phys. Rev. C **22**, 2287 (1980).

[12] D. L. Mason, M. L. Halbert, A. van der Woude, and L. C. Northcliffe, Phys. Rev. **179**, 940 (1969); D. O. Galde, M. L. Halbert, C. A. Ludemann, and A. van der Woude, Phys. Rev. Lett. **25**, 1581 (1970).

[13] An extensive list of references can be found in Ref. [24]. For the recent literature, see R. Bilger *et al.*, Phys. Lett. B **429**, 195 (1998); J. Zlomanczuk, A. Johansson, and the WASA-PROMICE Collaboration, Nucl. Phys. **A631**, 622c (1998); K. Yasuda *et al.*, Phys. Rev. Lett. **82**, 4775 (1999).

[14] An extensive list of references can be found in Ref. [24]. For the recent literature, see V. R. Brown, P. L. Anthony, and J. Franklin, Phys. Rev. C **44**, 1296 (1991); V. Hermann and K. Nakayama, *ibid.* **46**, 2199 (1992); A. Katsogiannis and A. Amos, *ibid.* **47**, 1376 (1993); J. A. Eden and M. F. Gari, Z. Phys. A **347**, 145 (1993); M. Jetter and H. V. von Geramb, Phys. Rev. C **49**, 1832 (1994); M. Jetter and H. W. Fearing, *ibid.* **51**, 1666 (1995); F. de Jong, K. Nakayama, and T.-S. Lee, *ibid.* **51**, 2334 (1995); F. de Jong and K. Nakayama, *ibid.* **52**, 2377 (1995); Phys. Lett. B **385**, 33 (1996); J. A. Eden and M. F. Gari, Phys. Rev. C **53**, 1102 (1996); G. Martinus, O. Scholten, and J. A. Tjon, *ibid.* **56**, 2945 (1997); **58**, 686 (1998).

[15] M. K. Liou, R. Timmermans, and B. F. Gibson, Phys. Rev. C **54**, 1574 (1996).

[16] M. K. Liou, R. Timmermans, and B. F. Gibson, Phys. Lett. B **345**, 372 (1995); **355**, 606(E) (1995). On p. 375, the statement "In contrast, M_μ^{TsTts} is evaluated at two energies and four angles, ..." is incorrect; it should read "In contrast, M_μ^{TsTts} is evaluated at two energies and two angles using the TETAS approximation, ..." The two-energy–four-angle approximations suffer the phase-space problem, while the two-energy–two-angle approximation is free of such a problem. See the Appendix of this paper as well as Ref. [27] for further discussion.

[17] Yi Li, M. K. Liou, and W. M. Schreiber, Phys. Rev. C **57**, 372 (1995); M. K. Liou, Yi Li, W. M. Schreiber, and R. W. Brown, *ibid.* **52**, R2346 (1995).

[18] M. L. Goldberger, M. T. Grisaru, S. W. MacDowell, and D. Y. Wong, Phys. Rev. **120**, 2250 (1960).

[19] V. G. J. Stoks, R. A. M. Klomp, M. C. M. Rentmeester, and J. J. de Swart, Phys. Rev. C **48**, 792 (1993); M. C. M. Rentmeester, R. G. E. Timmermans, J. L. Friar, and J. J. de Swart, Phys. Rev. Lett. **82**, 4992 (1999).

[20] See on the world wide web, http://NN-OnLine.sci.kun.nl

[21] F. E. Low, Phys. Rev. **110**, 974 (1958).

[22] M. K. Liou, Phys. Rev. D **18**, 3390 (1978).

[23] M. K. Liou and Z. M. Ding, Phys. Rev. C **35**, 651 (1987).

[24] M. K. Liou, D. Lin, and B. F. Gibson, Phys. Rev. C **47**, 973 (1993).

[25] M. K. Liou, R. Timmermans, B. F. Gibson, and Yi Li, Phys. Rev. C **60**, 039801 (1999).

[26] M. Welsh and H. W. Fearing, Phys. Rev. C **54**, 2240 (1996).

[27] Z. M. Ding, Dahang Lin, and M. K. Liou, Phys. Rev. C **40**, 1291 (1989).

[28] Dahang Lin, M. K. Liou, and Z. M. Ding, Phys. Rev. C **44**, 1819 (1991), and references cited therein.

[29] D. Yan, P. M. S. Lesser, M. K. Liou, and C. C. Trail, Phys. Rev. C **45**, 331 (1992), and references therein.

[30] H. Feshbach and D. R. Yennie, Nucl. Phys. **37**, 150 (1962).

[31] K. Michaelian *et al.*, Phys. Rev. D **41**, 2689 (1990).

[32] D. Drechsel and L. C. Maximon, Ann. Phys. (N.Y.) **49**, 403 (1968).